CHINESE OPTICS LETTERS

Vol. 20, No. 11 | November 2022

Fabrication and characterization of on-chip silicon spherical-like microcavities with high Q-factors

Hailong Han (韩海龙)[1,2], Hao Li (李 浩)[1,2], Lixing You (尤立星)[1,2], and Xiaoping Liu (刘晓平)[3*]

[1] State Key Laboratory of Functional Materials for Informatics, Shanghai Institute of Microsystem and Information Technology (SIMIT), Chinese Academy of Sciences (CAS), Shanghai 200050, China

[2] CAS Center for Excellence in Superconducting Electronics (CENSE), Shanghai 200050, China

[3] School of Physical Science and Technology, ShanghaiTech University, Shanghai 201210, China

*Corresponding author: liuxp1@shanghaitech.edu.cn

Received April 13, 2022 | Accepted June 6, 2022 | Posted Online July 13, 2022

An effective way to fabricate high-quality (Q) silicon microcavities on-chip is proposed and studied. Our fabrication technique consists of two significant steps: (1) patterning a special silicon micro-pillar by Bosch processes and (2) subsequent reflow of the pillar into a spherical-like microcavity using a laser pulse at 532 nm. Its shape and surface roughness are characterized using a scanning electron microscope and an atomic force microscope. The root-mean-square roughness of the surface is about 0.6 nm. A representative value for the loaded Q-factors of our silicon spherical-like microcavities is on the order of 10^5.

Keywords: optical microcavity; whispering gallery mode; high Q-factor.

DOI: 10.3788/COL202220.111301

1. Introduction

Optical microcavities have attracted considerable attention and played an essential role in on-chip classic and quantum information processing during the past decades[1,2]. Optical microcavities have broad application areas, such as micro-lasers[3], channel-adding-and-dropping filters[4,5], optical switching[6], ultrafine sensing[7], displacement measurement[8], and rotation detection[9]. High-quality (Q) optical microcavities with a Q-factor $> 10^7$ are mostly made from silica using techniques such as reflow and sophisticated etching to create wedged facets[10]. They have been molded into a wide variety of forms, from spheres[11] and toroids[12] to disks[13], bottles[14], rings[15], and bubbles[16]. However, the transparent window for silica is limited in the visible and near-infrared regions. There are enormous vital applications in the mid-infrared area, where optical microcavities can be leveraged. Silicon happens to be a transparent optical medium from near-infrared up to 8 μm in the mid-infrared region[17,18], and it has a substantial nonlinear coefficient (e.g., its third-order nonlinearity susceptibility is 10^3 times larger than that of silica)[19]. Therefore, silicon is an excellent candidate for optical microcavities and resultant cavity-enhanced nonlinear applications in this wavelength region. Using a sophisticated dry or wet etching process, silicon microrings, microdisks, and microspheres have been reported[20–22]. Moreover, silicon microspheres have been obtained by chemical vapor deposition techniques. Still, their sizes are too small to be used as high-Q-factor optical microcavities for the near-infrared and mid-infrared regions[23]. Hung *et al.* used the high-power excimer laser to melt and reshape the silicon rods to obtain spheres of larger sizes. However, the spheres have maximum size restrictions because of the limited thermal conduction rate[24]. In another experiment, Wu *et al.* fabricated silicon microspheres by melting the silicon strip with a hydrogen torch, and the Q-factor obtained in their work was 1.3×10^4[25]. Li *et al.* fabricated micrometer and submicrometer (200–1000 nm) silicon spheres by pulsed-laser selective heating in a liquid medium[26]. Many efforts have been devoted to reducing the scattering losses caused by surface roughness, including dry oxidation, wet chemical etching, and hydrogenation[27–29]. However, achieving relatively large silicon spherical cavities while having high Q-factors remains a big challenge.

We propose fabricating on-chip silicon spherical microcavities by heating a large silicon pillar on a silicon pedestal or a mushroom-like silicon structure on a silicon-on-insulator (SOI) substrate with a laser under atmospheric pressure and at room temperature. Different etching processes are used in our experiment to prepare these unique structures; a careful direct laser-heating step with proper influence then reshapes these mushroom-like structures into spherical microcavities by reflowing the whole structure. The exact shape and morphology of the prepared silicon spherical microcavities are characterized using a scanning electron microscope (SEM) and an atomic

© 2022 Chinese Optics Letters

force microscope (AFM). Optical whispering gallery modes (WGMs) of these spherical microcavities are tested using a tapered-fiber coupling system, in which a loaded-Q on the order of 10^5 is demonstrated.

2. Experiment

Our experiment fabricated silicon spherical microcavities on a commercial SOI wafer with a 16-μm-thick device layer and a 2-μm-thick buried oxide. The device layer is n-type silicon with orientation (100) and resistance of 10–20 Ω·cm. Instead of using a single silicon pillar, a mushroom-like structure, where a silicon pillar sits on a narrow pedestal, as shown in Fig. 1, is used to fabricate a spherical microcavity by reflowing. The reason for not using a single pillar is that reflowing such a structure in experiments makes it difficult to form a spherical shape due to silicon's low surface tension. Two-step Bosch processes with different process parameters are adopted in a sequence to prepare the mushroom-like structure. A Bosch process requires two kinds of gases, where the SF_6 gas does the etching while C_4F_8 gas deposits a passivation layer to inhibit the already etched and exposed sidewall. A very deep silicon etching could be achieved periodically by alternating these two gases. The etched sidewall is usually not perfectly vertical microscopically, but instead, it is curvy because of the tendency of isotropic etching and periodic along the vertical etching direction because of the periodic alternation of two gases. Usually, with a considerable period, the sidewall becomes increasingly curvy. This effect is exploited to make a unique mushroom-like silicon structure by tuning different time ratios between etching and passivation.

Detailed step-by-step fabrication processes are presented in Fig. 1. First, the commercial SOI wafer mentioned above is cleaned and spin-coated with a layer of photoresist (AZ5214) about 1.5 μm thick and then patterned with a mask-less photolithography system (SF-100, Intelligent). Second, after development, the first Bosch process is performed in the HSE200s Deep Silicon Etcher. The top part of a mushroom-like structure, a silicon pillar, forms after 60 cycles of Bosch processes. The size of this pillar primarily determines the size of the spherical microcavity prepared later by laser reflowing. Third, another Bosch process is used to prepare the pedestal of the mushroom-like structure by first depositing a thick passivation layer on the already formed silicon pillar to prevent it from being further etched. Next, the pillar is undercut to create a narrow pedestal via a relatively long etching time to complete the mushroom-like structure. The main parameters of two different Bosch processes are listed in Table 1. Finally, a direct laser-heating step with an adequately controlled influence reshapes the mushroom-like structure to a more-or-less spherical silicon microcavity with the help of silicon surface tension in its liquid state during heating. An optical laser beam with a wavelength of 532 nm and an emission power of 5 W (Coherent Verdi V18), which silicon strongly absorbs, is focused onto the fabricated structure with an estimated optical intensity of $16\,\mathrm{MW/cm^2}$. A programmable shutter is used to precisely control the laser illumination time. After several rounds of optimization, a suitable illumination time for our structure is determined to be about 0.005 s. The energy density imposed on this structure is estimated to be $80\,\mathrm{J/cm^2}$.

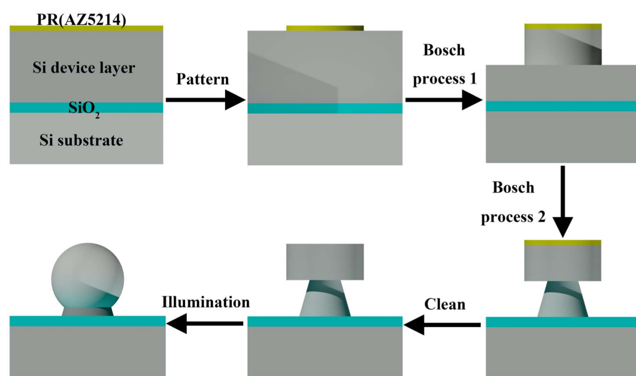

Fig. 1. Flowchart of the fabrication processes.

Table 1. Main Parameters of Bosch Processes.

1st Bosch Process		2nd Bosch Process	
Passivation time/cycle	Etching time/cycle	Passivation time/cycle	Etching time/cycle
0.8 s	1.7 s	7 s	24.5 s
Number of cycles: 60		Number of cycles: 1	

3. Results and Discussion

The exact shapes of our fabricated on-chip samples before and after 532 nm laser illumination are characterized using SEM and shown in Fig. 2. A side review of an as-etched sample shown in Fig. 2(a) reveals the mushroom-like structure. Further investigations show that this pillar has a diameter of about 15 μm and a height of about 6.5 μm. Figures 2(b) and 2(c) show the silicon structure's front and top views after laser illumination. The newly formed structure has a nearly spherical shape except for the north pole region, which has a noticeable bump. A strong correlation is found between the location of this bump and the moving direction of the blade inside the shutter during the closing of the shutter. It is thus suspected that the bump is the last part of the silicon spherical-like structure to solidify during the sudden cooling down caused by the laser illumination being blocked by the shutter. The low surface tension of silicon cannot completely smooth the surface before the structure solidifies. The low surface tension is also responsible for the unsuccessful attempts of forming a silicon sphere when only a silicon pillar without a pedestal is used for laser heating and reflow. It is found experimentally in this case that only a half-sphere could be

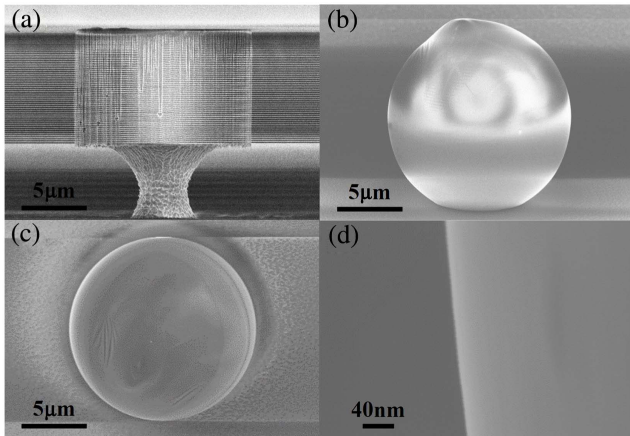

Fig. 2. SEM images of our prepared sample. (a) Side view before laser illumination, (b) and (c) side view and top view after laser illumination, and (d) zoom-in view of the edge after laser illumination.

formed. However, without a clearly defined equator, this half-sphere does not support high-Q optical WGMs. To solve this issue, the current mushroom-like structure is developed, and, with it, the formed spherical-like silicon structure has an exposed equator zone with a diameter measured to be close to 15 μm. Figure 2(d) shows the zoom-in SEM view of the details of the surface of the sphere-like silicon microcavity near the equator region. The overall surface Q is excellent, judging from its surface smoothness.

To further investigate its surface Q, AFM is utilized to observe the surface morphology of this fabricated silicon sphere-like microcavity, and a representative AFM image for regions near the equator is shown in Fig. 3. The root-mean-square (RMS) roughness, calculated from the measured data, is only about 0.6 nm. As a comparison, the surface roughness of the commercially available polished Si substrate is about 0.2 nm[30]. Therefore, the surface-tension-induced surface reformation process can achieve superb surface smoothness using the laser reflow technique. As a result, this could potentially give rise to very low optical scattering loss and enables high-Q-factor WGMs.

The resonance spectrum and Q-factor of our silicon sphere-like microcavities' modes are characterized via an evanescent coupling method using an optical fiber taper[31]. Our experimental setup is similar to that in Ref. [25]. A super-luminescent emitted diode laser (China-Fiber, Model: OS-EB-D-1250–1650-1-FC/APC) and an optical spectrum analyzer (Yokogawa, Model: AQ6375B) are used to measure the transmission spectrum from the fiber taper with a wavelength resolution bandwidth of 0.05 nm and a wavelength sampling resolution of 2 pm. The fiber taper formed by heating and stretching a section of a commercial optical fiber (Corning, SMF-28) has a minimum waist diameter of approximately 1.5 μm, providing an evanescent excitation of WGMs of the cavity. To facilitate the coupling of light into the on-chip microcavities with a fiber taper and ensure that the silicon spherical microcavities are at the edge of the chip, we dice the wafer into individual sample chips using the laser-dicing machine (ML200PLUS, Tokyo Seimitsu Co., Ltd.). A dual CCD camera observation configuration is used to image the microcavity simultaneously and the fiber taper from the side and the top to make sure the position of the fiber taper is near the equator of the silicon sphere-like structure. Optical coupling to the microcavity from the fiber taper is achieved and tuned by moving the on-chip microcavity fixed on an XYZ three-axis piezo nano-positioning stage. The transmission spectrum for a silicon sphere-like microcavity with a diameter of 14.37 μm is recorded when the overall resonances are at their most distinct states.

Figure 4(a) shows a section for the wavelength range from 1515 to 1525 nm. The resonances of the WGMs of the silicon

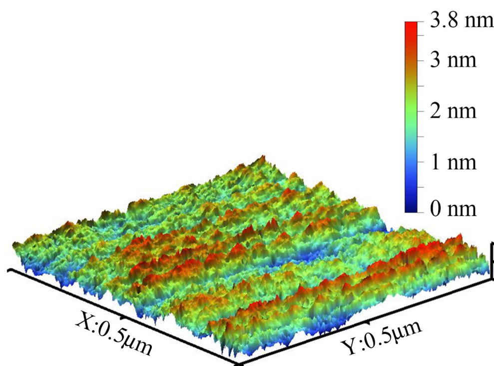

Fig. 3. AFM image of the fabricated silicon spherical microcavity.

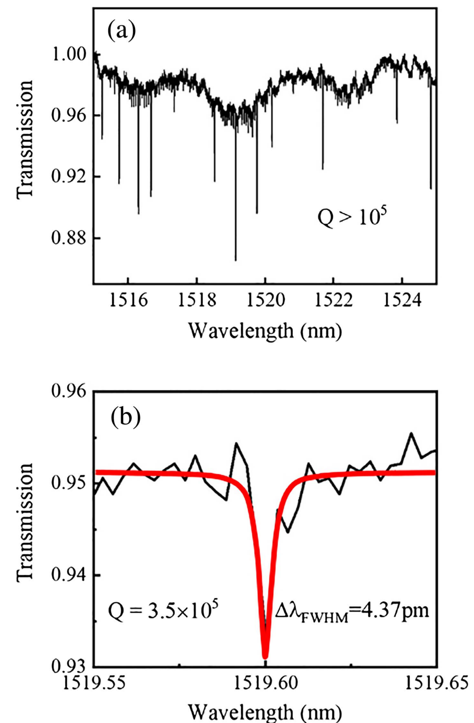

Fig. 4. (a) Transmission spectrum of the microcavity coupled with the fiber taper from 1515 to 1525 nm; (b) the Lorentzian fit (solid red line) of the measured spectrum around the resonant wavelength at 1519.6 nm (solid black line), showing a Q-factor of 3.5×10^5.

sphere-like microcavity are observed as the corresponding Lorentzian dip families in the shown spectrum. The Q-factor is defined as the ratio of the energy stored in the oscillating cavity to the energy dissipated per cycle by damping processes[32], which can be expressed by $Q = \lambda/\Delta\lambda$, where λ is the central wavelength of a WGM, and $\Delta\lambda$ is its full width at half-maximum. Due to the large effective index mismatch between the WGMs of this silicon microcavity and the silica fiber taper, the resonance mode is under coupled, and its strength is relatively weak. Nevertheless, the measured loaded Q-factors for these WGMs are still on the order of 10^5. An individual WGM located at 1519.6 nm, as shown in Fig. 4(b), is chosen for further analysis. By fitting the experimental data using a Lorentzian function (the red curve)[25], the linewidth is found to be as small as 4.37 pm, and thus the loaded Q-factor for the mode is calculated to be 3.5×10^5. Considering that this linewidth is comparable to the wavelength sampling resolution in measurement, we suspect that the extracted Q-factor here is instrumentally limited. The actual intrinsic Q-factor may be much higher than this. Nevertheless, the results here show that our method for preparing the silicon sphere-like microcavities possesses the potential to enable low surface-scattering loss and high-Q WGM resonances.

4. Conclusions

In conclusion, we have proposed and demonstrated a method to fabricate high-Q-factor on-chip silicon sphere-like microcavities by laser heating a particular mushroom-like silicon structure. To fabricate such structures, two different Bosch processes are developed. With the illumination of an intense 532 nm laser beam, this particular structure can be melted and reshaped into a silicon sphere-like microcavity, which has a clear exposed equator that can be used to exploit WGMs. The advantage of this method is apparent in that it allows for fabricating relatively large microcavities and, importantly, gives rise to a minimal surface RMS roughness, only about 0.6 nm. This, in turn, leads to WGM resonances with instrumentally limited loaded Q-factors above 10^5. We believe that this fabrication method may open new avenues for cost-effective large-area processing of complex three-dimensional (3D) optical cavity structures and promises great potential in nonlinear light–matter interactions.

Acknowledgement

This work was supported by the Zhejiang Key Research and Development Program (No. 2021C01188), the start-up funding from ShanghaiTech University, and the Shanghai Municipal Science and Technology Major Project (No. 2017SHZDZX03).

References

1. K. J. Vahala, "Optical microcavities," Nature **424**, 839 (2003).
2. J. Ward and O. Benson, "WGM microresonators: sensing, lasing and fundamental optics with microspheres," Laser Photonics Rev. **5**, 553 (2011).
3. M. Cai, O. Painter, K. J. Vahala, and P. C. Sercel, "Fiber-coupled microsphere laser," Opt. Lett. **25**, 1430 (2000).
4. T. Bilici, S. Isci, A. Kurt, and A. Serpengüzel, "Microsphere-based channel dropping filter with an integrated photodetector," IEEE Photon. Tech. Lett. **16**, 476 (2004).
5. M. Cai, G. Hunziker, and K. J. Vahala, "Fiber-optic add-drop device based on a silica microsphere-whispering gallery mode system," IEEE Photon. Technol. Lett. **11**, 686 (1999).
6. H. C. Tapalian, J. P. Laine, and P. A. Lane, "Thermooptical switches using coated microsphere resonators," IEEE Photon. Technol. Lett. **14**, 1118 (2002).
7. I. Teraoka, S. Arnold, and F. Vollmer, "Perturbation approach to resonance shifts of whispering-gallery modes in a dielectric microsphere as a probe of a surrounding medium," J. Opt. Soc. Am. B **20**, 1937 (2003).
8. J. P. Laine, C. Tapalian, B. Little, and H. Haus, "Acceleration sensor based on high-Q optical microsphere resonator and pedestal antiresonant reflecting waveguide coupler," Sens. Actuators A Phys. **93**, 1 (2001).
9. A. B. Matsko, A. A. Savchenkov, V. S. Ilchenko, and L. Maleki, "Optical gyroscope with whispering gallery mode optical cavities," Opt. Commun. **233**, 107 (2004).
10. H. Lee, T. Chen, J. Li, K. Y. Yang, S. Jeon, O. Painter, and K. J. Vahala, "Chemically etched ultrahigh-Q wedge-resonator on a silicon chip," Nat. Photonics **6**, 369 (2012).
11. M. L. Gorodetsky, A. A. Savchenkov, and V. S. Ilchenko, "Ultimate Q of optical microsphere resonators," Opt. Lett. **21**, 453 (1996).
12. D. K. Armani, T. J. Kippenberg, S. M. Spillane, and K. J. Vahala, "Ultra-high-Q toroid microcavity on a chip," Nature **421**, 925 (2003).
13. R. Schilling, H. Schütz, A. H. Ghadimi, V. Sudhir, D. J. Wilson, and T. J. Kippenberg, "Near-field integration of a SiN nanobeam and a SiO_2 microcavity for Heisenberg-limited displacement sensing," Phys. Rev. Appl. **5**, 054019 (2016).
14. M. Pöllinger, D. O'Shea, F. Warken, and A. Rauschenbeutel, "Ultrahigh-Q tunable whispering-gallery-mode microresonator," Phys. Rev. Lett. **103**, 053901 (2009).
15. S. I. Shopova, H. Zhou, X. Fan, and P. Zhang, "Optofluidic ring resonator based dye laser," Appl. Phys. Lett. **90**, 221101 (2007).
16. Y. Yang, S. Saurabh, J. M. Ward, and S. N. Chormaic, "High-Q, ultrathin-walled microbubble resonator for aerostatic pressure sensing," Opt. Express **24**, 294 (2016).
17. R. Shankar, R. Leijssen, I. Bulu, and M. Lončar, "Mid-infrared photonic crystal cavities in silicon," Opt. Express **19**, 5579 (2011).
18. C. Reimer, M. Nedeljkovic, D. J. M. Stothard, M. O. S. Esnault, C. Reardon, L. O'Faolain, M. Dunn, G. Z. Mashanovich, and T. F. Krauss, "Mid-infrared photonic crystal waveguides in silicon," Opt. Express **20**, 29361 (2012).
19. G. P. Agrawal, *Nonlinear Fiber Optics*, 2nd ed. (Academic, 1995).
20. S. A. Miller, M. Yu, X. Ji, A. G. Griffith, J. Cardenas, A. L. Gaeta, and M. Lipson, "Low-loss silicon platform for broadband mid-infrared photonics," Optica **4**, 707 (2017).
21. K. Srinivasan, H. X. Miao, M. T. Rakher, M. Davanco, and V. Aksyuk, "Optomechanical transduction of an integrated silicon cantilever probe using a microdisk resonator," Nano Lett. **11**, 791 (2011).
22. M. Garín, R. Fenollosa, R. Alcubilla, L. Shi, L. Marsal, and F. Meseguer, "All-silicon spherical-Mie-resonator photodiode with spectral response in the infrared region," Nat. Commun. **5**, 3440 (2014).
23. R. Fenollosa, F. Meseguer, and M. Tymczenko, "Silicon colloids: from microcavities to photonic sponges," Adv. Mater. **20**, 95 (2008).
24. S. C. Hung, S. C. Shiu, C. H. Chao, and C. F. Lin, "Fabrication of crystalline Si spheres with atomic-scale surface smoothness using homogenized KrF excimer laser reformation system," J. Vac. Sci. Technol. B **27**, 1156 (2009).
25. J. Wu, Y. Huang, Y. Lin, Q. Li, J. Huang, T. Wu, and C. Guo, "Whispering gallery modes from silicon microsphere in C-band," IEEE Photon. Technol. Lett. **27**, 1993 (2015).
26. X. Li, A. Pyatenko, Y. Shimizu, H. Wang, K. Koga, and N. Koshizaki, "Fabrication of crystalline silicon spheres by selective laser heating in liquid medium," Langmuir **27**, 5076 (2011).
27. J. Takahashi, T. Tsuchizawa, T. Watanabe, and S. Itabashi, "Oxidation-induced improvement in the sidewall morphology and cross-sectional profile of silicon wire waveguides," J. Vac. Sci. Technol. B **22**, 2522 (2004).
28. D. K. Sparacin, S. J. Spector, and L. C. Kimerling, "Silicon waveguide sidewall smoothing by wet chemical oxidation," J. Light. Technol. **23**, 2455 (2005).

29. H. Kuribayashi, R. Hiruta, R. Shimizu, K. Sudoh, and H. Iwasaki, "Shape transformation of silicon trenches during hydrogen annealing," J. Vac. Sci. Technol. A **21**, 1279 (2003).
30. H. Hara, Y. Sano, K. Arima, K. Yagi, J. Murata, A. Kubota, H. Mimura, and K. Yamauchi, "Catalyst-referred etching of silicon," Sci. Technol. Adv. Mater. **8**, 162 (2007).
31. J. C. Knight, G. Cheung, F. Jacques, and T. A. Birks, "Phase-matched excitation of whispering gallery modes by a fiber taper," Opt. Lett. **22**, 1129 (1997).
32. Y. Chen, Y. Yin, L. Ma, and O. G. Schmidt, "Recent progress on optoplasmonic whispering-gallery-mode microcavities," Adv. Opt. Mater. **9**, 2100143 (2021).